

Model-Based Analysis of Membrane-Enhanced Liquid-Phase Oligonucleotide Synthesis^{*}

Alberto Saccardo^{*} Benoît Chachuat^{*}

^{*} *The Sargent Centre for Process Systems Engineering, Department of Chemical Engineering, Imperial College London, UK*

Abstract: Oligonucleotides show great promise for therapeutic applications. While traditional solid-phase oligonucleotide synthesis presents manufacturing challenges due to low scalability, lack of real-time monitoring and high process mass-intensity, liquid-phase synthesis (LPOS) combined with soluble anchors and membrane diafiltration has emerged as a viable alternative. Herein, we formulate a multi-stage dynamic model of the LPOS process using a multi-branched homostar support hub. We exploit this model to analyse the interplay between the durations of the reaction and diafiltration steps on the oligonucleotide yield and purity through the solution of an inverse feasibility problem.

Keywords: Oligonucleotide, liquid-phase synthesis, phosphoramidite chemistry, diafiltration, organic solvent nanofiltration, mathematical modelling, feasibility analysis

1. INTRODUCTION

Oligonucleotides are short sequences of nucleic acids (DNA or RNA), typically comprising around 20 nucleotides. They belong to the class of oligonucleotides and peptides (TIDES) therapeutic drugs and have the potential to treat or manage a wide range of diseases (Roberts et al., 2020). During the period 2016–2023, 16 new oligonucleotide drugs have received approval from the US Food and Drug Administration (FDA) (Al Shaer et al., 2024), and the global market for these therapeutics is projected to grow from US\$5.2 Bn in 2020 to US\$26.1 Bn by 2030 (Ferrazzano et al., 2023).

Despite their recognised therapeutic potential, the market share for oligonucleotide drugs remains modest, representing only 4% of the FDA-approved drugs between 2016–2023. This limited share is also attributed to challenges in the manufacturing process (Ferrazzano et al., 2023). Solid-phase oligonucleotide synthesis (SPOS) is a well-established method, wherein phosphoramidites are sequentially added to a growing chain immobilised on a solid support (Pichon and Hollenstein, 2024). However, this technique has notable caveats due to its low scalability (producing batches under 10 kg), no possibility of real-time process monitoring, and a staggering process mass intensity (PMI) of over 4000 kg of waste per kg for a 20-building block oligonucleotide (Andrews et al., 2021).

To address these challenges, innovative approaches like membrane-enhanced liquid-phase oligonucleotide synthesis (LPOS) are being actively researched (Chen et al., 2017, 2018). In LPOS, oligonucleotides are supported on a

soluble anchor and iteratively undergo reaction and diafiltration steps to remove byproducts and excess reagents through organic solvent nanofiltration (OSN). This approach enables a tighter control over the nucleotide sequence compared to solid-phase synthesis (Kim et al., 2016). Additionally, the use of a branched *homostar* to support multiple chains significantly reduces oligonucleotide losses during diafiltration (Gaffney et al., 2015). The homogeneous nature of LPOS can further overcome the mass transfer limitations present in SPOS, enabling effective scale-up for large-scale production (Kim et al., 2016).

Despite its technological potential, membrane-enhanced LPOS remains in an early stage of development. In particular, the LPOS process is inherently multistage and discontinuous, with key process variables in each stage impacting the overall production performance. To pave the way to industrial-scale production, it is essential to better understand the sensitivity of these process variables and their interplay on oligonucleotide production yield and purity. Mathematical modelling can be of great assistance in this context.

There is currently no mathematical model describing the LPOS process with homostar supports. The objective of this paper, therefore, is to develop a first dynamic model of LPOS. Then, we exploit this model to analyse the interplay between key operational decisions in LPOS on the yield and purity of oligonucleotides.

2. BACKGROUND AND METHODOLOGY

2.1 Process Description

The membrane-enhanced LPOS process (Gaffney et al., 2015; Kim et al., 2016) comprises three main phases: (i) initial loading of the support hub, (ii) chain extension by iterative addition of building blocks to the homostar

^{*} This work was supported by Innovate UK under grant number 10103756 (Sustainable bioprocess for oligonucleotide manufacture using Nanostar Sieving – BioNanostar). Correspondence should be directed to Benoît Chachuat: b.chachuat@imperial.ac.uk

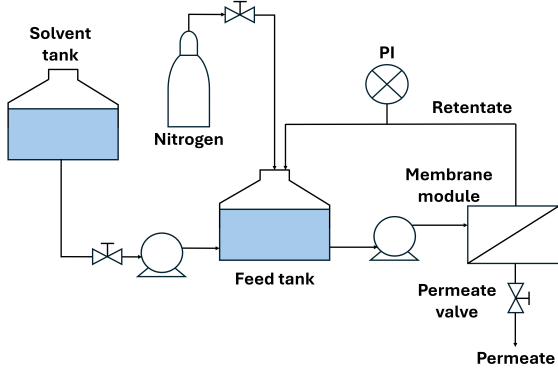


Fig. 1. Process layout (adapted from Kim et al., 2016).

branches, and (iii) final cleavage and purification of the oligonucleotides. The focus of this paper is on developing a mathematical model for the second phase.

The addition of each building block entails a four-step cycle, which is repeated until the desired nucleotide sequence is obtained. The first step (*deprotection* or *detritylation*) removes the protection group from the growing chain to enable its reaction with the building block. The temporary protecting group in the N-terminus (Dmtr) is removed catalytically with trifluoroacetic acid (TFA). Following detritylation, TFA and the cleaved protection groups are removed through constant-volume diafiltration in the second step, while the homostars are retained on the retentate side. In the third step (*coupling*), specific nucleotides with a temporary protecting group are added as building blocks via conventional phosphoramidite chemistry. To facilitate the reaction with the deprotected chains on the homostar branches, dicyanoimidazole (DCI) and camphorsulfonyl oxaziridine (CSO) are also added. The outcome is a series of longer, protected chains attached to the homostar branches. After this coupling, cyanoethanol is used to quench the reaction, deactivating the building block to prevent side reactions from occurring in subsequent cycles. This is followed by a second diafiltration in the final step, which removes reaction byproducts and any unreacted reagents (building blocks, DCI, CSO), again to prevent interference with the oligomers in subsequent coupling reactions.

In the actual process (Figure 1), reagents are added to a feed tank at the start of the reaction steps. The mixture is continuously recirculated in the retentate during the reaction (without running the membrane filtration). During the diafiltration steps, solvent is added to the feed tank to continuously replace the volume passed through the membrane.

Since molecular structure determines the biological functions of oligonucleotides, tight control over the sequence during the polymerisation is essential. In particular, sequence errors occurring during the coupling step reduce product purity. For a target sequence A–B–C, the main types of error include truncated (A–B), deleted (A–C), and repeated (A–B–B) sequences (Chen et al., 2017). A key advantage of LPOS is that such sequence errors can be controlled through careful tuning of the reaction and diafiltration times. Moreover, the use of multibranching homostars enables higher yields by increasing the size

differential with the building blocks, thus reducing product loss through the membrane.

2.2 Process Modeling

Our mathematical model of LPOS builds upon an existing model of liquid-phase peptide synthesis (Chen et al., 2017, 2018), adapted to describe oligonucleotide synthesis and enable the use of multibranching homostar supports. It assumes constant volume for both the retentate and permeate sides. Since the solution is continuously recirculated on the retentate side and accumulated on the permeate side during diafiltration, both sides are furthermore modelled as well-mixed vessels.

For a desired product sequence with N building blocks, N cycles of deprotection-diafiltration-coupling-diafiltration are required. During each cycle $n = 1 \dots N$, the relevant building block is added to the growing oligonucleotides, with its molar concentration denoted as BB_n (mol m^{-3}). Similarly, the concentrations of the deprotected/protected anchored oligonucleotide of length n —both without and with sequence error—are denoted as OD_n and OP_n , respectively, while OD_0 and OP_0 refer to the supports without any nucleotide attached. The total concentration of all anchored oligonucleotides OT (mol m^{-3}) is given by

$$OT(t) = \sum_{n=0}^N OP_n(t) + OD_n(t). \quad (1)$$

Note that OP_n , OD_n and OT all refer to concentrations in the mixture volume on the retentate side of the membrane. All of these concentrations are initially set to zero, except for that of protected supports, given by

$$OP_0(0) = HS \cdot NB, \quad (2)$$

with HS (mol m^{-3}) the total concentration of homostar supports and NB the number of branches on the supports.

The combination of mass conservation equations in each step of each cycle results in a multistage dynamic model, with possible state discontinuities at the transitions between steps. These systems of equations are specified in the following paragraphs, before stating the process performance indicators of interest.

Deprotection Step. The deprotection reaction during cycle n consumes any protected anchored oligonucleotides of length $k = 0 \dots n - 1$ to produce their deprotected counterparts, according to

$$\dot{OD}_k(t) = -\dot{OP}_k(t) = k_D OP_k(t) TFA(t) \quad (3)$$

where k_D ($\text{m}^3 \text{mol}^{-1} \text{s}^{-1}$) is the deprotection kinetic constant and TFA (mol m^{-3}) the concentration of TFA in the retentate. Since the latter acts catalytically in the deprotection reaction, its concentration remains constant throughout a deprotection step, following a pulse addition TFA^{in} (mol m^{-3}) at the corresponding start time $t_{D,n}$,

$$TFA(t) = TFA(t_{D,n}^+) = TFA(t_{D,n}^-) + TFA^{\text{in}}. \quad (4)$$

The concentrations of all the other species in the mixture not participating in deprotection remain constant.

Coupling Step. The coupling reaction during cycle n consumes any deprotected (anchored) oligonucleotides of length $k = 0 \dots n - 1$ and appends the relevant building

blocks to form new protected oligonucleotides of length $k + 1$, according to the apparent stoichiometric reaction



The case $k = n$ refers to the coupling yielding the desired oligonucleotide sequence of length n . The other cases $k < n$ describe truncated/deleted sequence errors, whereby a shorter oligonucleotide—resulting from a previous incomplete coupling—is being extended with the current building block. In particular, the corresponding variables OD_k, OP_{k+1} will comprise different types of oligonucleotides, all considered as impurities since representing an incorrect sequence. On the other hand, repeating sequences—caused by coupling reactions with residual building blocks BB_k from a previous cycle—are neglected since (i) residual building blocks are deactivated through quenching at the end of the coupling step (Székely et al., 2014) and (ii) the concentration of previous building blocks will be extremely low after undergoing deactivation and two diafiltrations during each cycle.

Material balances for protected and deprotected anchored oligonucleotides are given by

$$\begin{aligned} \dot{OP}_{k+1}(t) &= -\dot{OD}_k(t) \\ &= k_C BB_n(t) OD_k(t) DCI(t) CSO(t) \end{aligned} \quad (6)$$

where DCI and CSO (mol m^{-3}) are the concentrations of DCI and CSO, respectively, and k_C ($\text{m}^9 \text{mol}^{-3} \text{s}^{-1}$) the apparent kinetic constant for the coupling reaction. Corresponding material balances for the building blocks, DCI and DSO account for the coupling reactions of anchored oligonucleotides of different lengths $k = 0 \dots n - 1$ as well as a side reaction between the building blocks and CSO, with apparent kinetic constant k_S ($\text{m}^3 \text{mol}^{-1} \text{s}^{-1}$),

$$\begin{aligned} \dot{BB}_n(t) &= \dot{DCI}(t) = \dot{CSO}(t) \\ &= k_C BB_n(t) \sum_{k=0}^{n-1} OD_k(t) DCI(t) CSO(t) \\ &\quad - k_S BB_n(t) CSO(t). \end{aligned} \quad (7)$$

Moreover, pulse additions of building blocks BB^{in} and reactants $DCI^{\text{in}}, CSO^{\text{in}}$ (mol m^{-3}) are made at the start time $t_{C,n}$,

$$BB_n(t_{C,n}^+) = BB_n(t_{C,n}^-) + BB^{\text{in}} \quad (8)$$

$$DCI_n(t_{C,n}^+) = DCI_n(t_{C,n}^-) + DCI^{\text{in}} \quad (9)$$

$$CSO_n(t_{C,n}^+) = CSO_n(t_{C,n}^-) + CSO^{\text{in}}. \quad (10)$$

The concentrations of all the other species in the mixture not participating in coupling remain constant, identical to those in the previous step.

Diafiltration Steps. A constant-rejection model (Kim et al., 2013) is used to describe the transport of a solute of concentration X (mol m^{-3}) through the OSN membrane,

$$\dot{X}(t) = -\frac{Q}{V} (1 - r_X) X(t) \quad (11)$$

where V (m^3) denotes the liquid volume on the retentate side. The volumetric transmembrane flux Q ($\text{m}^3 \text{s}^{-1}$) is calculated as

$$Q = A K \Delta p \quad (12)$$

where K is the membrane permeability ($\text{m s}^{-1} \text{bar}^{-1}$), A (m^2) the membrane area, Δp (bar) the transmembrane pressure difference. For simplicity, the observed rejection

Table 1. Design and model parameter values.

Parameter	Nominal value
HS	5.0 mol m^{-3}
NB	4
k_D	$3.6 \times 10^{-5} \text{ m}^3 \text{mol}^{-1} \text{s}^{-1}$
k_C	$2.7 \times 10^{-8} \text{ m}^9 \text{mol}^{-3} \text{s}^{-1}$
k_S	$4.3 \times 10^{-6} \text{ m}^3 \text{mol}^{-1} \text{s}^{-1}$
BB^{in}	1.5 eq^\dagger
TFA^{in}	8.0 eq^\dagger
DCI^{in}	4.0 eq^\dagger
CSO^{in}	6.0 eq^\dagger
A	$8.5 \times 10^{-2} \text{ m}^2$
V	$9 \times 10^{-4} \text{ m}^3$
Δp	8.9 bar
K	$5.6 \times 10^{-7} \text{ m s}^{-1} \text{bar}^{-1}$
r_{OP}	0.998
r_{OD}	0.998
r_{BB}	0.40
r_{TFA}	0.33
r_{DCI}	0.33
r_{CSO}	0.33

[†] Equivalent amounts relative to the initial total amount of anchored oligonucleotides $OT(0) = HS \cdot NB$.

r_X (–) of solute $X = OP_k, OD_k, BB_k, TFA, DCI, CSO$ is assumed constant during diafiltration. The same rejection is furthermore assumed for protected or deprotected anchored oligonucleotides of various lengths and types,

$$r_{OP_k} = r_{OD_k}, \quad \forall k. \quad (13)$$

This is motivated by the fact that the transport properties are not so specific to a particular anchored oligonucleotide but to the support hub instead, whose size is significantly larger than the other solutes (Székely et al., 2014).

Key Performance Indicators. We assess the LPOS process in terms of three performance indicators. The *overall yield*, Y (–) is the ratio of (anchored) oligonucleotides with correct sequence after N cycles to the theoretical maximum,

$$Y = \frac{OP_N(t_{F2,N}^-)}{HS \cdot NB}. \quad (14)$$

Any loss of anchored oligonucleotides through the membrane during diafiltration and any truncated/deleted sequence errors will reduce this yield.

The *product purity*, P (–) is the ratio of oligonucleotides with correct sequence to all oligonucleotides after N cycles,

$$P = \frac{OP_N(t_{F2,N}^-)}{OT(t_{F2,N}^-)}. \quad (15)$$

Both incomplete coupling reactions and sequence errors will be detrimental to the purity.

The *maximal building block residue*, R (–) is calculated as the maximum of ratios between residual building blocks and total oligonucleotides after the first diafiltration over all cycles,

$$R = \max_{n=1 \dots N} \frac{\sum_{k=1}^n BB_k(t_{C,n}^-)}{OT(t_{C,n}^-)}. \quad (16)$$

Keeping this ratio low prevents unwanted side reactions from occurring in future coupling cycles and is in agreement with typical process control strategies.

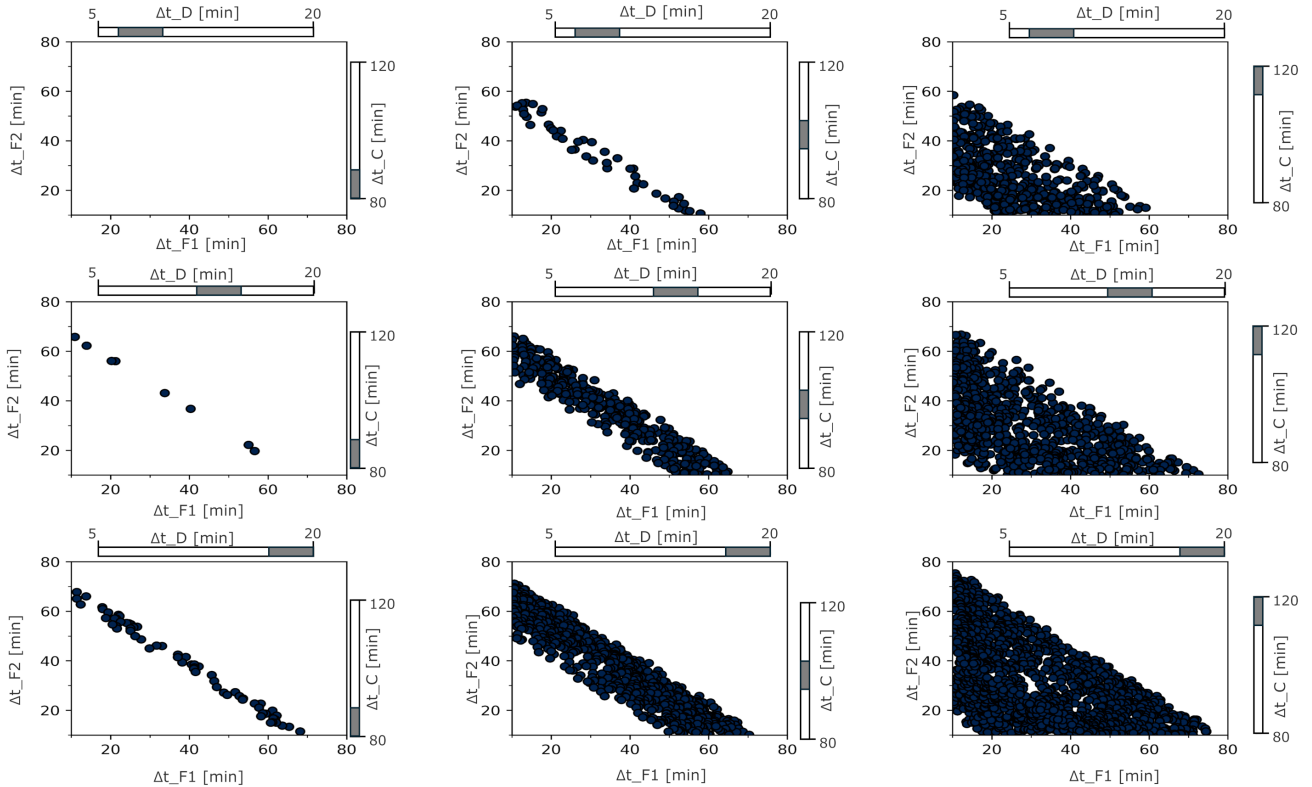


Fig. 2. Sampled feasible operating region (blue points) for meeting the process targets $Y \geq 0.9$, $P \geq 0.9$ and $R \leq 0.01$, computed using nested sampling with 10 000 live points and 3000 replacement proposals.

2.3 Feasible Operating Space Characterisation

Our model-based analysis is aimed at better understanding the interplay between key operational decisions on achieving high yield and purity in LPOS. The focus is on four operational decisions, namely the lengths of the deprotection (Δt_D), coupling (Δt_C), diafiltration (Δt_{F1} , Δt_{F2}) stages; while the performance indicators of interest were defined earlier and include the overall yield (Y), product purity (P), and maximal building block residue (R).

Since the LPOS model is at an early stage of development, we gathered an initial set of parameter values from our industrial partner (Exactmer Ltd.) and recent literature (Chen et al., 2018) in Table 1. We conduct a nominal feasibility analysis on this basis, which entails computing a subset of operating parameter combinations (Δt_D , Δt_{F1} , Δt_C , Δt_{F2}) from a given prior set such that the performance indicators (Y , P , R) remain within set limits, either simultaneously or separately. Future work will estimate some of the uncertain model parameters (e.g., kinetic constants and observed rejections) from experimental using maximum likelihood or Bayesian estimation and will, in turn, investigate the use of probabilistic feasibility analysis techniques (Kusumo et al., 2020) to account for the presence of this parametric uncertainty.

We use an algorithm based on nested sampling, which is implemented in the Python package DEUS¹, to inner-approximate the feasible operating set (Paulen et al., 2020). This nested sampling adaptation proceeds by im-

proving a population of *live points*, until all the live points eventually become feasible. A number of replacement proposals are sampled from within regions that get iteratively closer to the desired feasibility region, based on a tailored likelihood function measuring a distance to this target region. Any replacement proposal with a likelihood higher than the current worst live point enters the live set, while the worst live point is dropped and becomes a *dead point*.

The tuning parameters that need to be set in DEUS to conduct a nominal feasibility analysis include: the number of live points, determining the resolution of the search; and the number of candidate replacements per iteration, as a means of balancing computational efficiency with exploration. The evaluation of all these points entails the numerical integration of the multistage dynamic model developed in Sec. 2.2, which was conducted using SciPy.

3. RESULTS AND DISCUSSION

3.1 Feasible Operating Set Analysis

To identify operating regions with high yield, high purity, and low building block residue, we conducted a nominal feasible space characterization. The feasibility targets were set to

$$Y \geq 0.9, \quad P \geq 0.9, \quad R \leq 0.01,$$

while the (a priori) operational ranges were defined as

$$5 \leq \Delta t_D \leq 20 \text{ min}, \quad 80 \leq \Delta t_C \leq 120 \text{ min}, \\ 10 \leq \Delta t_{F1}, \Delta t_{F2} \leq 80 \text{ min},$$

based on physical process insight. Figure 2 shows the results of the nested sampling algorithm in DEUS with

¹ <https://github.com/omega-ic1/deus>

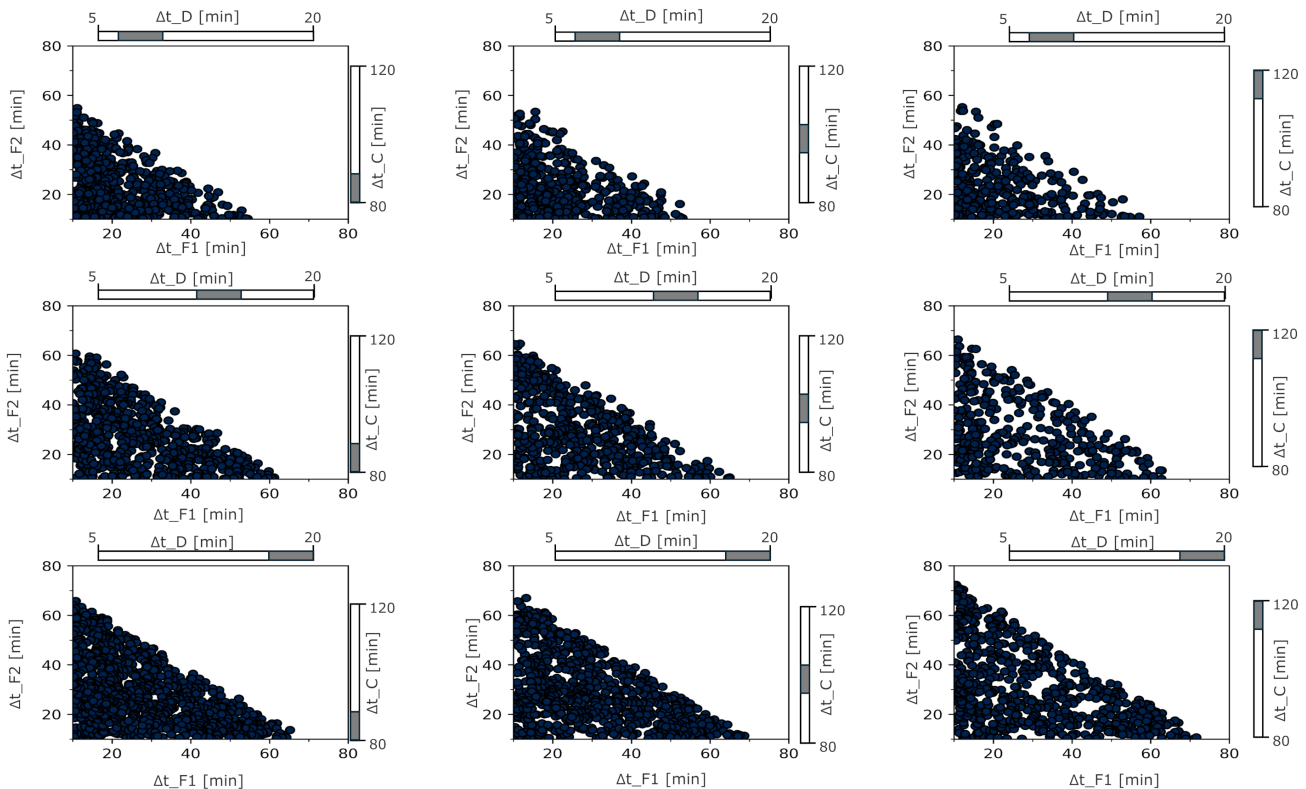


Fig. 3. Sampled feasible operating region (blue points) for meeting the purity target $Y \geq 0.9$, computed using nested sampling with 10000 live points and 3000 replacement proposals.

10000 live points and 3000 replacement points, where all the points are inside the joint feasible region. The 4-dimensional feasible region is represented on a trellis chart, where the inner axes on each subplot correspond to the diafiltration times Δt_{F1} , Δt_{F2} and the outer axes to the deprotection and coupling times Δt_D , Δt_C (with values indicated by the grey-shaded ranges).

Notice how the feasible region in Figure 2 is dictated by the combined diafiltration step duration $\Delta t_{F1} + \Delta t_{F2}$ being within certain bands. The position and extent of these bands depend on the deprotection and coupling step durations. For low values of Δt_D and Δt_C , the feasible region is empty or a narrow band. As Δt_D and Δt_C take larger values, this feasible band gets significantly wider, with a higher sensitivity attributed to increasing Δt_C . The existence of such a band can be attributed to the fact that insufficient lengths for the deprotection and coupling steps result in a higher level of truncated sequence errors, a greater concentration of unreacted building blocks in the retentate, and a lower overall yield.

To draw further process insight, Figures 3 and 4 plot the feasibility region corresponding to, respectively, the targets $Y \geq 0.9$ and $R \leq 0.01$ alone. In terms of meeting the overall yield target, longer diafiltration steps result in a greater loss of anchored oligonucleotides through the membrane. The feasibility region, therefore, is *upper-bounded* by the combined diafiltration duration $\Delta t_{F1} + \Delta t_{F2}$. This upper limit (between 60–75 min) increases with longer deprotection and coupling steps, since a greater loss through the membrane can then be compensated by a

higher conversion of oligonucleotides. However, it does not exhibit a high sensitivity within the investigated range of deprotection and coupling step durations, and even the shortest diafiltration steps (10 min) do not preclude an overall yield above 90%. In terms of meeting the maximal building block residue target, shorter diafiltration steps lead to greater residual concentration of building blocks. The situation, therefore, is the diametrical opposite, with the feasible region now *lower-bounded* by the combined diafiltration duration $\Delta t_{F1} + \Delta t_{F2}$. In particular, Δt_C appears to be highly sensitive as longer coupling steps increase building block consumption (either through reaction (5) or the side reaction with CSO), thereby reducing the reliance on diafiltration to eliminate the building block excess. Finally, in terms of meeting the purity target, the feasible region (not shown) is found to have the same shape of that of the yield, yet with a larger upper limit for the imposed 90% target. Overall, the trends observed on the joint feasible region in Figure 2 are essentially the intersection of the feasible regions in Figures 3 and 4 for meeting the 90% yield and 1% building block residue targets.

4. CONCLUSIONS

We presented a new multistage dynamic model to describe membrane-enhanced liquid-phase oligonucleotide synthesis (LPOS) using a homostar support hub. We then conducted a model-based feasibility analysis to draw process insight in terms of operational decisions. Our results suggest that the combined diafiltration duration within each cycle plays a key role in terms of ensuring a high

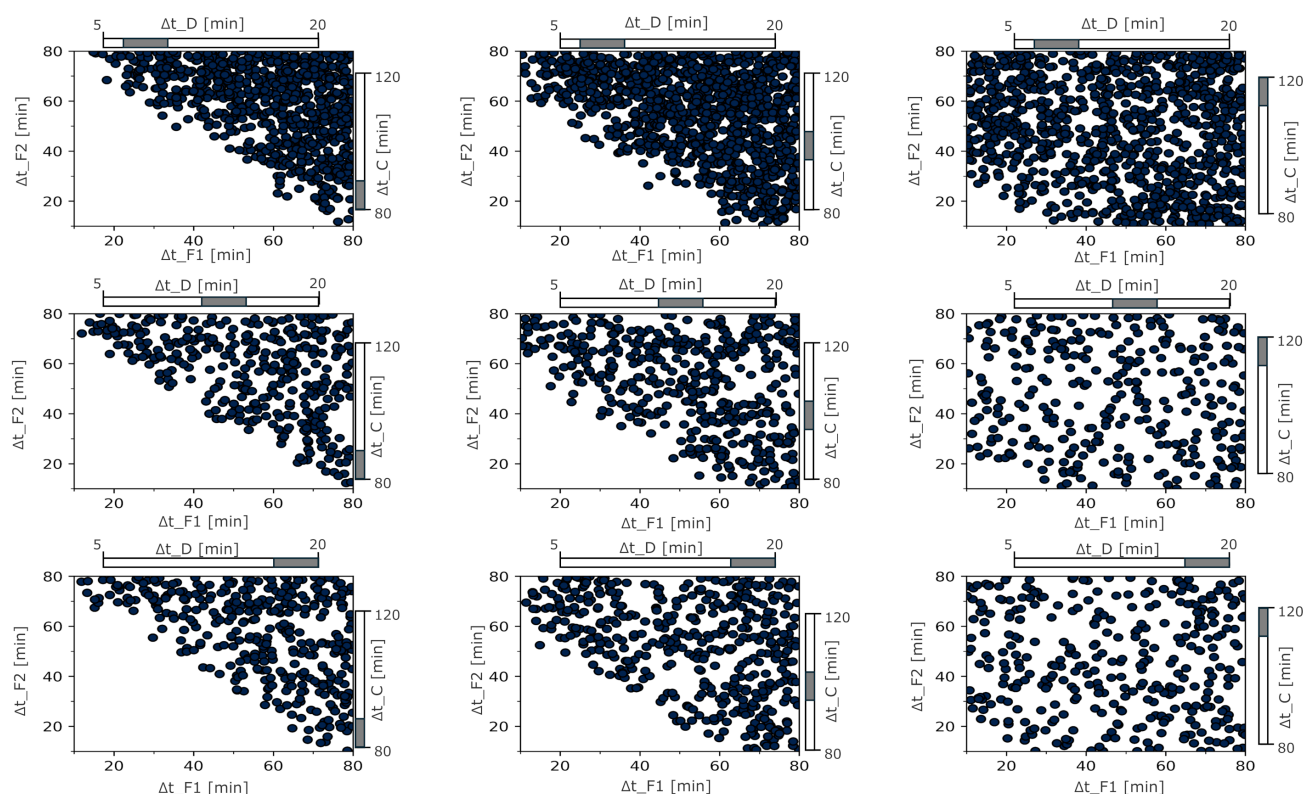


Fig. 4. Sampled feasible operating region (blue points) for meeting the building block residue target $R \leq 0.01$, computed using nested sampling with 10 000 live points and 3000 replacement proposals.

yield and purity of oligonucleotides, and present a strong interplay with the duration of the coupling step and, to a lower extent, with the duration of the deprotection step. Our next steps will entail calibrating and validating the dynamic model with experimental data to create a tool that practitioners can use for optimization and on-line monitoring and control of the LPOS process.

ACKNOWLEDGEMENTS

The authors gratefully acknowledge Exactmer Ltd. for providing them with information about the LPOS process.

REFERENCES

- Al Shaer, D., Al Musaimi, O., Albericio, F., and De La Torre, B.G. (2024). 2023 FDA TIDES (Peptides and Oligonucleotides) Harvest. *Pharmaceuticals*, 17(2), 243.
- Andrews, B.I., Antia, F.D., Brueggemeier, S.B., Diorazio, L.J., Koenig, S.G., Kopach, M.E., Lee, H., Olbrich, M., and Watson, A.L. (2021). Sustainability challenges and opportunities in oligonucleotide manufacturing. *The Journal of Organic Chemistry*, 86(1), 49–61.
- Chen, W., Sharifzadeh, M., Shah, N., and Livingston, A.G. (2017). Implication of side reactions in iterative biopolymer synthesis: The case of membrane enhanced peptide synthesis. *Industrial & Engineering Chemistry Research*, 56(23), 6796–6804.
- Chen, W., Sharifzadeh, M., Shah, N., and Livingston, A.G. (2018). Iterative peptide synthesis in membrane cascades: Untangling operational decisions. *Computers & Chemical Engineering*, 115, 275–285.
- Ferrazzano, L., Corbisiero, D., Tolomelli, A., and Cabri, W. (2023). From green innovations in oligopeptide to oligonucleotide sustainable synthesis: differences and synergies in TIDES chemistry. *Green Chemistry*, 25(4), 1217–1236.
- Gaffney, P.R.J., Kim, J.F., Valtcheva, I.B., Williams, G.D., Anson, M.S., Buswell, A.M., and Livingston, A.G. (2015). Liquid-phase synthesis of 2'-methyl-RNA on a homostar support through organic-solvent nanofiltration. *Chemistry – A European Journal*, 21(26), 9535–9543.
- Kim, J.F., Freitas Da Silva, A.M., Valtcheva, I.B., and Livingston, A.G. (2013). When the membrane is not enough: A simplified membrane cascade using organic solvent nanofiltration (OSN). *Separation and Purification Technology*, 116, 277–286.
- Kim, J.F., Gaffney, P.R.J., Valtcheva, I.B., Williams, G., Buswell, A.M., Anson, M.S., and Livingston, A.G. (2016). Organic solvent nanofiltration (OSN): A new technology platform for liquid-phase oligonucleotide synthesis (LPOS). *Organic Process Research & Development*, 20(8), 1439–1452.
- Kusumo, K.P., Gomoescu, L., Paulen, R., García Muñoz, S., Pantelides, C.C., Shah, N., and Chachuat, B. (2020). Bayesian approach to probabilistic design space characterization: A nested sampling strategy. *Industrial & Engineering Chemistry Research*, 59(6), 2396–2408.
- Paulen, R., Gomoescu, L., and Chachuat, B. (2020). Nested sampling approach to set-membership estimation. *IFAC-PapersOnLine*, 53(2), 7228–7233.
- Pichon, M. and Hollenstein, M. (2024). Controlled enzymatic synthesis of oligonucleotides. *Communications Chemistry*, 7(1), 138.
- Roberts, T.C., Langer, R., and Wood, M.J.A. (2020). Advances in oligonucleotide drug delivery. *Nature Reviews Drug Discovery*, 19(10), 673–694.
- Székely, G., Schaepertoens, M., Gaffney, P.R.J., and Livingston, A.G. (2014). Beyond PEG2000: Synthesis and Functionalisation of Monodisperse PEGylated Homostars and Clickable Bivalent Polyethyleneglycols. *Chemistry – A European Journal*, 20(32), 10038–10051.